INTERNATIONAL JOURNAL OF CONSERVATION SCIENCE
ISSN: 2067-533X Volume 17, Issue 2, 2026: 547-566 www.ijcs.ro
DOI: 10.36868/IJCS.2026.02.09

EFFECT OF DIFFERENT SOLVENTS ON ANTIMICROBIAL PROPERTIES OF NANOMATERIALS FOR ARCHAEOLOGICAL WOOD CONSERVATION IN THE NATIONAL POLICE MUSEUM, EGYPT

Abdelmoniem M. ABDELMONIEM[1*], Ali M. OMAR[2], Wael S. MOHAMED[3]

[1] Conservation Department, Faculty of Archaeology, Fayoum University, Fayoum, Egypt.
[2] Conservation Center, Grand Egyptian Museum, Egypt
[3] Polymer department, National Research Centre, Dokki – Giza – Egypt.

Abstract
This investigation aims to isolate and identify the wood's microbial infestation to determine the treatment options for these problems in the cavern beneath the National Police Museum in the Citadel of Sultan Salah al-Din al-Ayyubi. It could be achieved by evaluating the effect of different solvents (distilled water, ethanol, propanol, and butanol) on the antimicrobial properties of silver nanoparticles (Ag NPs), silica nanoparticles (SiO_2 NPs), titanium dioxide nanoparticles (TiO_2 NPs), and nano-chitosan (CS NP) was used with water only. The fungi were cultivated on cellulose agar, while bacteria were cultivated on nutrient agar. The bacteria were Micrococcus lutus, Streptomyces vinaceus, Microbacterium imperial, and Kacurin turfanensis, while the fungi were Aspergillus niger, Humicola fuscoatra, Alternaria alternata, and Penicillium oxalicum. The results showed that nano-chitosan showed the highest fungal inhibition (30 mm) for all isolated microbial organisms, followed by Ag NP in ethanol and Ag NP in propanol, whose effect was for all microbial organisms. Additionally, there was a negative result for Penicillium oxalicum and Humicola fuscorta. The moisture content of the standard sample was 5.8%, while that of the treated samples was between 9.45% and 13.3%. The FTIR analysis of wood showed the degradation by fungi. Nanomaterials were applied using a brush and spray. After applying nano-chitosan and nano-silver to the treated samples, it was demonstrated that the samples treated with nano-silver darkened and turned black. The results of the mechanical properties test indicated that the standard sample measured 2623.83 N, and the sample with the highest mechanical properties of the treated sample was nano-chitosan applied by spray, measuring 6800.23 N.

Keywords*: Wood; Bacteria; Fungi; Microcides; Nanomaterials; Ag NPs; SiO_2 NPs; TiO_2 NPs*

Introduction

One of the most recognizable structures in Islamic Cairo is the Citadel of Sultan Salah al-Din al-Ayyubi, often known as Saladin. It is one of the most remarkable defensive fortifications from the Middle Ages. Its advantageous position atop the Muqattam Hills provided it with a strong defensive posture as well as an unhindered, all-encompassing view of Cairo. Although it was not finished during his lifetime, Sultan Salah al-Din al-Ayyubi initially ordered the construction of a castle over the Muqattam Hills in 572 AH/ 1176 AD. It was accomplished during Sultan al-Kamel ibn al-Adel's (604 AH/1207 AD) reign when he made it the official residence of Egypt's rulers. Khedive Ismail relocated the official house to Abdeen Palace in the heart of Cairo

[1] * Corresponding author: ama63@fayoum.edu.eg

in the middle of the 1800s. Situated in the northern section of the Citadel, the National Police Museum is one of Egypt's historical museums. It honors the part the Egyptian police played in preserving the country's safety and security during many historical eras. The museum's concept was first presented in 1986 at Police Day celebrations. It was closed in 2008 to accommodate development but reopened in 2013. The museum is housed in a single structure, separated into several halls. The halls feature images and archaeological collectibles that illustrate the efforts of the Egyptian police and their ongoing struggle from the time of the ancient Egyptians to the modern era.

Chemically, wood is mainly composed of cellulose and hemicelluloses (polysaccharides like xylans, mannans, β-glucans, and xyloglucans) along with lignin, an organic polymer made up of three basic monomers: guaiacyl, syringyl, and p-hydroxyphenyl subunits [1]. The interior environment, the nutrients accessible from the materials themselves and the atmosphere, and the frequency of cleanings in the museum all influence the establishment and development of different fungal strains in museums [2], [3]. Organic materials can deteriorate very quickly as a result of fungal degradation [4]. Most cultural heritage objects consist of materials that can be subjected to biodeterioration [5], [6]. In museums and storage facilities, elements such as inadequate ventilation, pollutants, and abundant light can also foster the spread of bacteria and insects [7]. Wooden objects should be kept in a stable (controlled) environment throughout their display and storage because temperature, moisture, and lighting cause degradation mechanisms to be active [8]. The application of nanotechnology in wood science mainly increases the durability and stability of wood through impregnation, coating, and other processes. Moreover, nanoparticles can penetrate deep into the wood base due to their small size, changing the surface characteristics and various wood properties [9]. The biological deterioration of construction materials is one of the most significant problems in their practical application [10], [11]. Wood-destroying fungi degrade the structural constituents of wood (cellulose, hemicellulose, and lignin), decreasing the physical and mechanical properties and contributing to the discoloration of the wood. The parenchyma cells are the first to be penetrated by fungal hyphae, followed by all types of wood cells. This causes erosion that breaks down the cell walls [12]. The research aims to evaluate different solvents with nanomaterials in treating microbial infections isolated from archaeological wood, apply these materials to wood samples, and evaluate them.

Materials and Methods

A scientific approach to the preservation of wooden cultural material must include the identification of the wood species and the characterization of the weathering processes [13] (Fig. 1). Fungi-induced wood and wood product biodegradation is one of the world's most serious issues, particularly regarding historical artifacts. Their acts might result in prospective losses in the past [14], [15]. Samples were taken from different parts of the wood (Fig. 2).

Fig. 1. Façade of the National Police Museum in Salah al-Din Citadel in Cairo

Fig. 2. Basement below the museum

Due to their contamination, fungi contribute significantly to the destruction of cultural assets by promoting the deterioration of the materials used to create historical artifacts. For restorers, preventing fungus, treating infected objects, and preserving those objects are crucial [16].

Cultivation of Swabs

The swabs were cultivated on the microbial growth media (nutrient agar/cellulose agar) and incubated at 28-30°C for 3-21 days. The media were produced. After that, the microbial growth was looked at to finish the lab tests (Tables 1 and 2).

Table 1. Nutrient agar medium (Cowan, 1974)

Ingredient	g/L
Beef extract	10
Peptone	10
Sodium chloride	5
Agar	15
Distilled water	1L
pH	7.0

Table 2. Cellulose agar medium (Difco, 1984)

Ingredient	g/L
Cellulose	10
Sodium nitrate	2
Potassium dihydrogen phosphate	1
Potassium chloride	0.5
Magnesium sulphate	0.5
$FeSO_4.7H_2O$	0.0001
$CaCl_2$	0.0001
Agar	15
Distilled water	1L
pH	7.0

Moisture content

To determine the percentage of internal water content, the wood's internal water content was measured the wooden samples before and after treatment using an Extech MO210 Pocket Moisture Meter.

Digital Image Processing and 3D Surface Analysis

D-Stretch Fuji and ImageJ were used on microbial examination by providing essential image editing and quantitative analysis features in a non-destructive analysis Gwyddion is a software program that transforms two-dimensional scanning electron microscope (SEM) images into three-dimensional representations. This technology provides a more comprehensive understanding of the surface topography and structure of materials at a microscopic level and to evaluate the surface roughness variations before and after wood alteration.

Optical Microscope

The light microscopy (Carl Zeiss Axio vision order Ks300/4000 Release: 4.72 with analysis unit and digital camera Cam MRc5) was used to identify fungi and bacteria [17].and The surfaces of the wooden samples were examined using a USB digital microscope with a magnification range of 20× to 500×, as well as a stereo microscope (Zeiss Stereo Discovery V20, equipped with an AxioCam MRC5).

Scanning Electron Microscope attached with Energy Dispersive X-Ray (SEM-EDX)

The wooden samples were examined using a Quanta 250 FEG with SEM. The accelerating voltage was 30 kV, and the magnification was 500× [18]. Using an accompanying energy-dispersive X-ray spectrometer (EDX), the distribution of chemical components on the wood surface was examined [19], [20].

FTIR Analysis

Attenuated total reflection Fourier-transform infrared (ATR-FTIR) spectra were acquired using a Nicolet iN10 MX spectrometer (Thermo Fisher Scientific, Waltham, MA, USA). A total of 32 scans were performed at a resolution for every spectrum of the wood samples [21], [22].

Mechanical Properties

Mechanical properties of treated wood, such as bending strength or elasticity, were examined [23]. The AG-X20 KN Autograph tables – Top Type, Shimadzu, Japan—were used for evaluation of the mechanical properties of the treated samples.

Wooden Samples

The type of wood used in the ceiling and basement of the Police Museum was identified in a published study by the author, where it was found to be of the *Pinus halepensis* species [24]. Models were used in experimentation, and mock samples were prepared and gathered. To provide a more accurate replication of the original material, the wood samples were correctly sized at 2.5×2.5×2.5 cm for the fungal tests [25] (Fig. 3). To infect the wooden samples, after identifying the isolated organisms, they were cultivated on Nutrient agar and Cellulose agar media. The fungi and bacteria were subsequently isolated and cultured in a aqueous solution to prepare spore suspension. to ascertain how isolated microbes affect their deterioration. Five milliliters of each microbial isolate's spore suspension, containing 0.5x106CFU, were sprayed over the pieces to inoculate them. For two months, the infected contemporary items were kept at room temperature and between sixty and seventy percent humidity.

Fig. 3. Created experimental samples

Moisture Content

The internal water content of the wood was measured at several points to determine the percentage of internal water content using an Extech MO210 Pocket Moisture Meter.

Determination of Minimal Inhibitory Concentration (MIC) of Antimicrobial Agents against the Isolated Microorganisms

Four microbicides were utilized to test their impact against the confined microorganisms and determine their MIC [26]. They were Ag NPs, SiO_2 NPs, TiO_2 NPs, and CS NPs.

Production and Characterization of Nanoparticles

Many nanomaterials are used to inhibit microbial growth [33] The term "nano" refers to materials whose dimensions are less than 100 nm [16]. This nanotechnology improves the efficacy of treatment in avoiding colonization while reducing the number of biocides used [27]. The first sign of the synthesis of TiO_2-NPs is the color shift of the CFF from pale yellow to white after mixing with the metal precursor [28]. Chitosan provides antimicrobial properties, which can help prevent the growth of fungi and bacteria that can cause decay and discoloration in wood [29]. It is the second most abundant natural biopolymer derived from the exoskeletons of crustaceans and from the cell walls of fungi and insects [30]. The wood treatment with TiO_2 particles is efficient for the preservation of the wood against the brown rot fungus attack and the photodegradation without altering its natural colorimetric characteristics [31].

Preparation of nanoparticle suspensions:

Nanoparticle suspensions were prepared by dissolving 2 grams of each of nanosilver, nanosilica, and nanotitanium dioxide separately in an independent 100 mL of water, ethanol, propanol, or butanol. Each suspension was introduced to a 400-watt ultrasonic sonication process for 15 min.

Preparation of nanochitosan solution

Chitosan was in a 94 mL aqueous solution containing 1 mL acetic acid. Then, 5 mL of 0.25% sodium TTP solution was added to the chitosan solution under a 400-watt ultrasonic sonication process for 15 min. Chitosan nanoparticles were shaped spontaneously [32]. The formed nanoparticles were purified by centrifugation at 9,000 rpm for 30 min. Supernatants were discarded, and the chitosan nanoparticles were extensively rinsed with deionized distilled water to remove any sodium hydroxide and freeze-dried before further use or analysis (A. Abdelmoniem et al., 2024) (Table 3) (Fig. 4).

Table 3. Experimental materials for the resistance to microbial infection

No	Treatment with 2%	No	Treatment with 2%
1	Ag Np in Distilled water	**8**	SiO_2 Np in Butanol
2	Ag Np in Ethanol	**9**	TiO_2 Np in Distilled water
3	Ag Np in Propanol	**10**	TiO_2 Np in Ethanol
4	Ag Np in Butanol	**11**	TiO_2 Np in Propanol
5	SiO_2 Np in Distilled water	**12**	TiO_2 Np in Butanol
6	SiO_2 Np in Ethanol	**13**	CS NP in Distilled water
7	SiO_2 Np in Propanol		

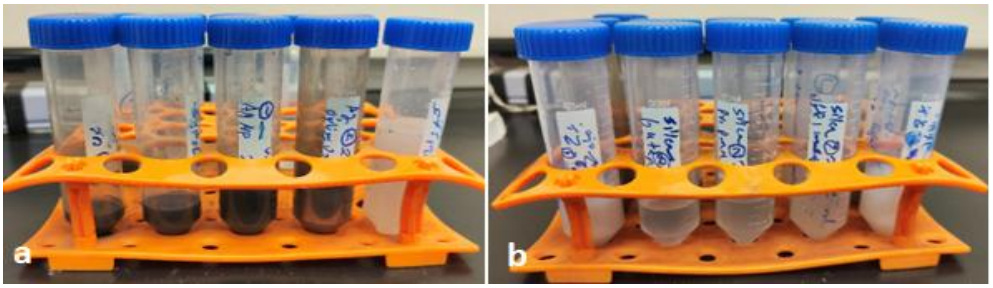

Fig. 4. Nanomaterials used to inhibit microbial growth: a) nano silver and nano Chitosan; b) nano silica

Results and Discussion

After the incubation period, microbial slides were made for each organism and examined using a light microscope. The morphological characteristics of each organism were determined and compared to the standard morphological characteristics found in books and scientific references used in defining microorganisms [34]. The results were as follows (Table 4, Figs. 5 and 6).

Table 4. Identification results of microbiological isolates

Media used	
Nutrient agar	Cellulose agar
Microbacterium imperial	*Aspergillus niger*
Micrococcus lutus	*Alternaria alternata*
Streptomyces vinaceus	*Penicillium oxalicum*
Kacurin turfanensis	*Humicola fuscorta*

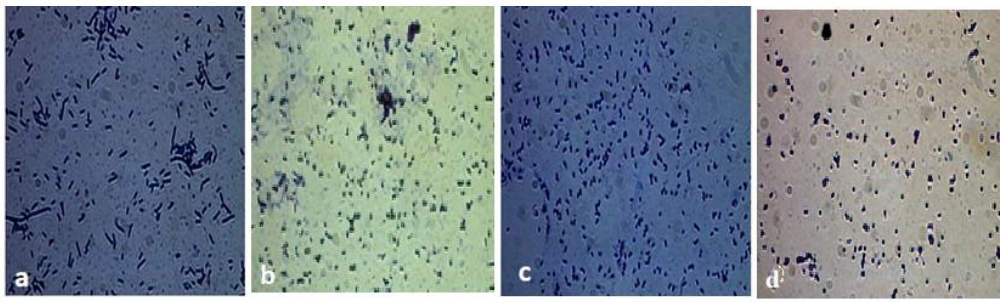

Fig. 5. Bacteria isolated from the wooden coffin:
a) *Bacillus megaterium;* b) *Micrococcus luteus, c) Microbacterium imperial; d) Kacurin turfanensis*

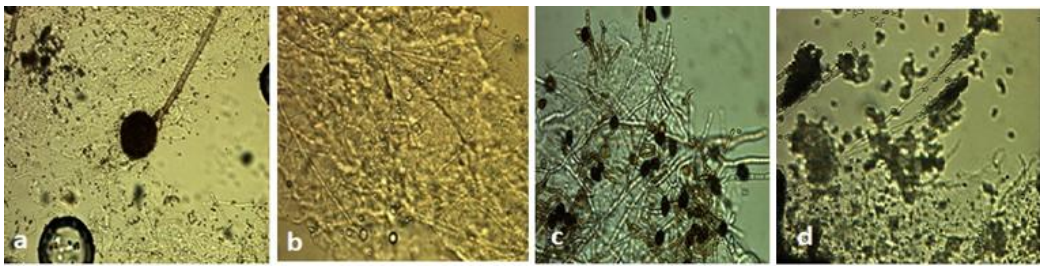

Fig. 6. Fungi isolated from the wooden coffin:
a) *Asp. Niger; b) Humicola fuscoatra; c) Alter. Alternaria; d) Penicillium oxalicum*

Microbial damage in the basement below the Police Museum may result from the high humidity, limited natural ventilation, and the lack of devices to control temperature and humidity. Fungal Decay: Due to the chemical composition and structural characteristics of wood, different fungi have varying capacities to degrade it. Enzymes produced by fungi attack the wood's cell walls to start the degradation process. While most wood-rotting fungi can break down cellulose and lignin, their degradation rates vary. The resulting decay patterns depend on the type of decay and the growth characteristics of the microorganisms in wood. Wood undergoes various physical, chemical, and morphological changes depending on the type of decay. Therefore, wood rotters are divided into three distinct decay groups based on the macroscopic variations in how they use their substrate: white rot, brown rot, and soft rot fungi [35], [36], [37].

CS NP in distilled water gave the best result in resisting isolated microbial organisms: *Micrococcus lutus* (55 mm), *Streptomyces vinaceus* (70 mm), *Microbacterium imperial* (65 mm), *Aspergillus niger* (23 mm), *Penicillium oxalicum* (28 mm), and *Humicola fuscorta* (30 mm).

It was followed by Ag Np in ethanol and Ag Np in propanol, whose effect was in ethanol: *Micrococcus lutus* (40 mm), *Streptomyces vinaceus* (50 mm), *Microbacterium imperial* (30 mm), and *Aspergillus niger* (24 mm); and in propanol: *Micrococcus lutus* (50 mm), *Streptomyces vinaceus* (45 mm), *Microbacterium imperial* (35 mm), and *Aspergillus niger* (22 mm). They both gave negative results for *Penicillium oxalicum* and *Humicola fuscorta* (Table 5).

Table 5. Antimicrobial agent's minimum inhibitory concentration (MIC) against isolated bacteria

Diameter of the clearing zone (mm)							
No	Microorganism / Nanomaterials	*Micrococcus lutus*	*Streptomyces vinaceus*	*Microbacterium imperial*	*Aspergillus niger*	*Penicillium oxalicum*	*Humicola fuscorta*
1	Ag Np in Distilled Water	**40**	**50**	**26**	**20**	**-ve**	**-ve**
2	Ag Np in Ethanol	**45**	**50**	**30**	**24**	**-ve**	**-ve**
3	Ag Np in Propanol	**50**	**45**	**35**	**22**	**-ve**	**-ve**
4	Ag Np in Butanol	**40**	**35**	**35**	**20**	**-ve**	**-ve**
5	SiO_2 Np in Distilled Water	**28**	**45**	**30**	**19**	**-ve**	**-ve**
6	SiO_2 Np in Ethanol	**30**	**30**	**25**	**18**	**-ve**	**-ve**
7	SiO_2 Np in Propanol	**25**	**30**	**19**	**-ve**	**-ve**	**-ve**
8	SiO_2 Np in Butanol	**20**	**29**	**22**	**-ve**	**-ve**	**-ve**
9	TiO_2 Np in Distilled Water	**21**	**30**	**-ve**	**-ve**	**-ve**	**-ve**
10	TiO_2 Np in Ethanol	**25**	**29**	**20**	**-ve**	**-ve**	**-ve**
11	TiO_2 Np in Propanol	**-ve**	**20**	**-ve**	**-ve**	**-ve**	**-ve**
12	TiO_2 Np in Butanol	**-ve**	**25**	**-ve**	**-ve**	**-ve**	**-ve**
13	CS NP in Distilled Water	**55**	**70**	**65**	**23**	**28**	**30**

TiO_2 NPs in ethanol and TiO_2 NPs in propanol were the least effective against *Micrococcus luteus* (25 mm), *Streptomyces vinaceus* (29 mm), *and Microbacterium imperiale (20 mm).* In contrast, the other microbial infection demonstrated negative results for *Aspergillus niger*, *Penicillium oxalicum, and Humicola fuscorta*. In propanol, the result was *Streptomyces vinaceus* (20 mm). Other isolated microbial infections showed negative results (Fig. 7).

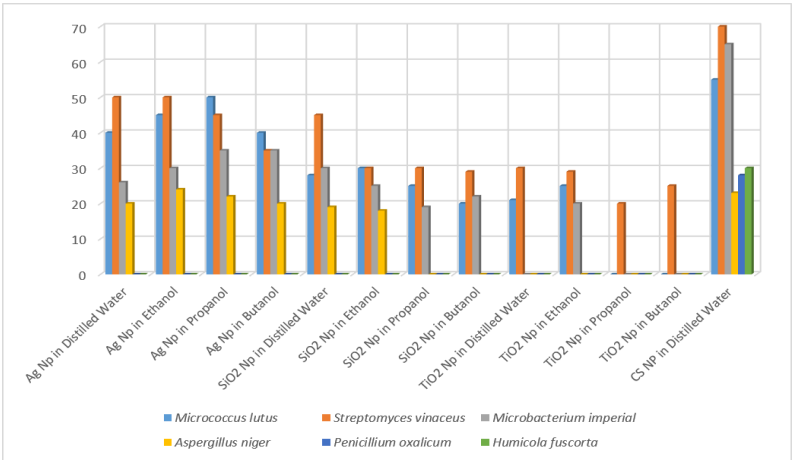

Fig. 7. A brief statistical analysis of the materials' efficacy in treating the wood

The best results were for nano-chitosan in distilled water and nano-silver in ethanol and propanol. Therefore, they were applied to 8 experimental wood samples: One standard sample without infection, an infected sample without treatment, and six samples in which the nanomaterial was applied by spraying to the sample and the other sample. The three materials were brushed on the samples to compare them as the best way to apply nanomaterials to wooden surfaces (Table 6).

Table 6. Samples and application methods

No	*Sample*	*Application Method*
1	*Standard sample without infection*	-----
2	*Standard sample with infection*	-------
3	Ag-Np in Ethanol	*Spray*
4	Ag-Np in Ethanol	*Brush*
5	Ag-Np in Propanol	*Spray*
6	Ag-Np in Propanol	*Brush*
7	CS NP in Distilled Water	*Spray*
8	CS NP in Distilled Water	*Brush*

Fig. 8. The wooden samples after infection

Microbial infection covered the surface of the wooden samples from all directions (Fig. 8).

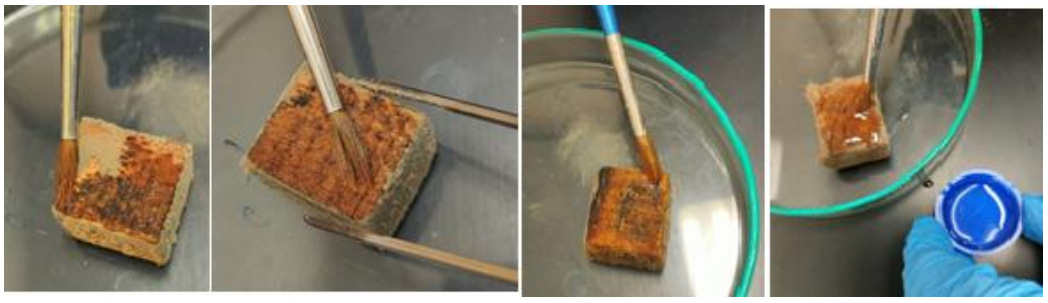

Fig. 9. During the application of nanomaterials on the wooden samples by brush

A quantity of the nanomaterial used for sterilization was put in a small plastic bottle and applied with a brush, ensuring that the entire solution was not disturbed. Moreover, a sprayer was used to spray the nanomaterial on the infected samples. During the application, it was noted that the spraying method consumed more materials than the brush method. Additionally, chitosan was slower to absorb into the sample than the second nanomaterial (Figs. 9 and 10).

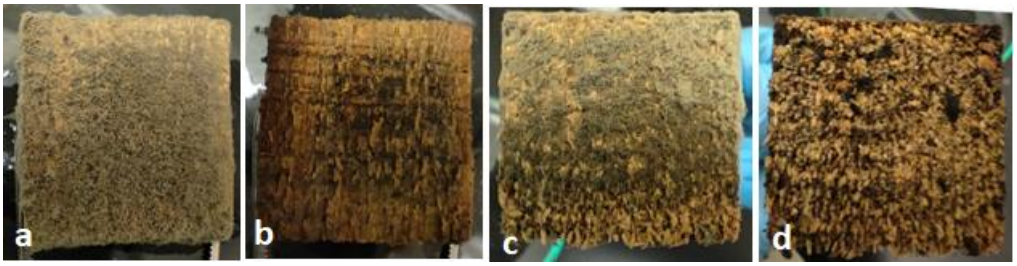

Fig. 10. Wooden sample replicas: a and c) Infected samples; b and d) after applying nanomaterials by spray

After 5 days of applying the nanomaterials by spraying and brushing, areas of the samples were taken and planted in dishes containing the media. Some growth was observed. Consequently, the nanomaterials were reapplied to the samples, and the samples were re-evaluated.

Fig. 11 shows the wooden samples: the infected samples showed clear infectation (fig. 11.a); the control samples (fig. 11.b); the samples sprayed with nano-chitosan (fig. 11.c); the sample treated with nano-chitosan by brush (fig. 11.d); the samples treated with nano silver in ethanol by spray (fig. 11.e); the samples treated with nano silver in propanol by spray (fig. 11.f, fig. 11.g); and the sample treated by brush (fig. 11.h). The wooden sample treated with nanosilver showed a clear color change as the color became dark.

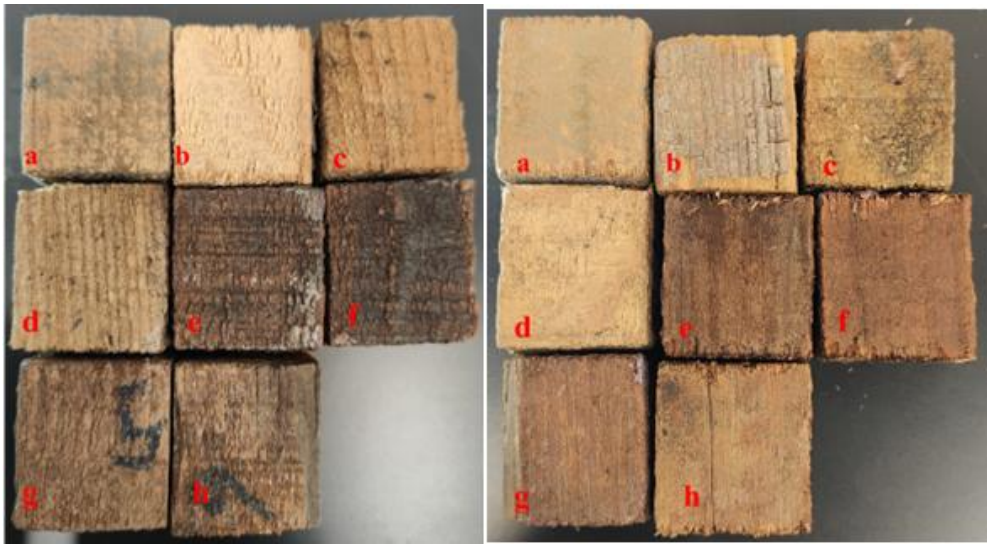

Fig. 11. The photos of the wooden samples: a) infected. b) Control; c) CS NP by spray; d) CS NPS by brush; e) Ag-Np in ethanol by spray; f) Ag-Np in ethanol by brush; g) Ag Np in propanol by spray; h) AgNp in propanol by spray

Fig. 12. Wooden samples replica: a) after treatment;
b) the effect of the Dstretch YDS filter on the treated wooden samples

The YDS filter in the Dstretch program for the treated wooden samples shows fluorescence on the infected sample. The standard sample and the samples treated with nanochitosan showed a clear darkening of the samples treated with nanosilver, which tended to be purple (Fig. 12).

Optical photomicrographs of the wooden samples

The control sample showed the effect of various forms of damage, such as microcracks and dust calcifications. Additionally, the infected sample illustrated that the fungi covered the surface of the samples (fig. 13). The samples treated with nanochitosan by spray displayed no traces of organisms (Fig. 14.a) because of the effect of the spray force resulting from the treatment process. The sample (Fig. 14.b) shows that when treated with nanochitosan by brush, there were some traces of fungi.

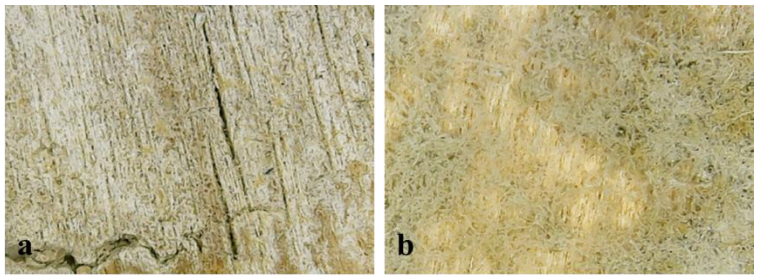

Fig. 13. Optical photomicrographs of the surface of the wooden samples; a) control; b) infected

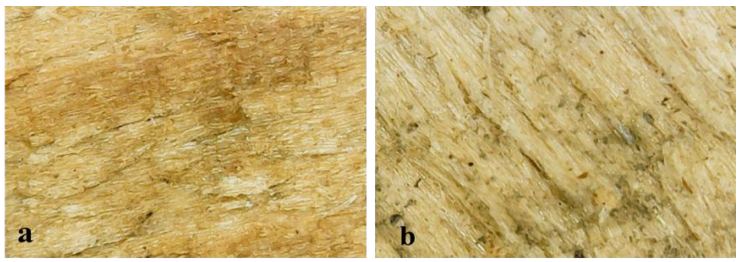

Fig. 14. Optical photomicrographs of the surface of the wooden samples; a) CS NPS; a) spray; b) brush

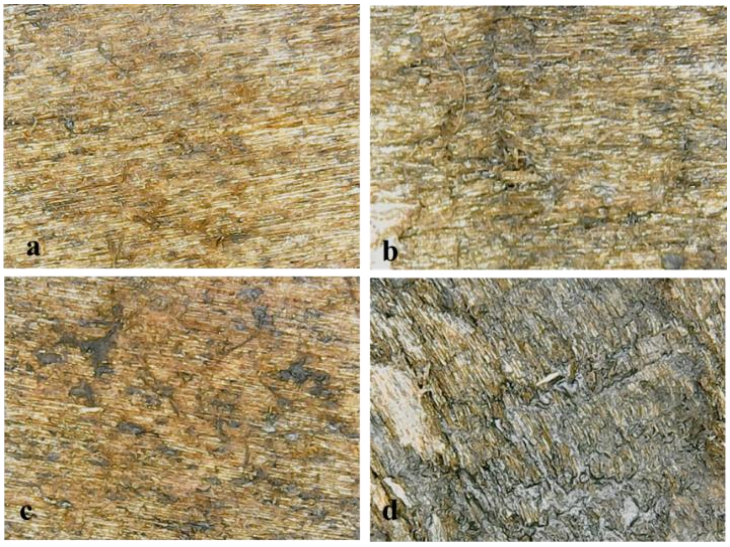

Fig. 15. Optical photomicrographs of the surface of the wooden samples:
a and b) Ag NPS in ethanol; c and d) spray; b) brush

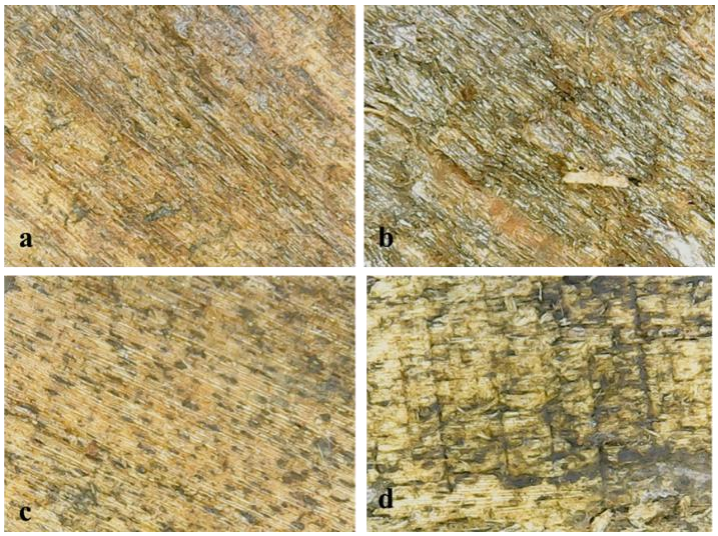

Fig. 16. Optical photomicrographs of the surface of the wooden samples:
a and b) Ag NPS in propanol; c and d) spray; b) brush

In the samples treated with nanosilver, the spray method was better than the brush in distributing the nanomaterials on the surface of the wooden samples (Fig. 15a and b, Fig. 16c-d), as the spraying process works to remove some fungal infections due to the pressure resulting from the spraying process. When applied using a brush (Fig. 15.c-d, Fig. 16.c-d), the nanomaterial particles appear to gather in the depressions on the surface. Thus, the materials can show the effect of nanosilver on the surface. The optical photomicrograph of the wooden sample treated with Ag Np in ethanol by brush showed that it was covered evenly with a nanosilver brush. It illustrated that the sample surface became dark due to the accumulation of silver nanoparticles on it (Fig. 17).

Fig. 17. Optical photomicrographs of the treated samples by Ag Np in ethanol by brush

Moisture Content

To achieve the highest possible infection of the wood samples, the moisture content of the infected wood samples was increased when measured 21 days after treatment. The moisture content of the standard sample was 5.8%, while the internal water content of the treated samples ranged from 9.45% to 13.3%.

Samples	Average of Humidity
Control	5.8
Infected	13.3
Nanochitosan by Spray	12.6
Nanochitosan by Brush	12.7
Nanosilver Ethanol by Spray	12.2
Nanosilver Ethanol by Brush	11.7
Nanosilver propanol by Spray	9.5
Nanosilver propanol by Brush	11.85

The average moisture content of wooden samples was 5.8% for the control samples and 13.3% for the infected samples because water by spray was added to the sample to improve the fungal growth. It was 12.7% for the samples treated with chitosan by brush. The highest moisture content was in the treated samples by nanochitosan by spray (12.6%), followed by the nanosilver in ethanol by spray (12.2%), silver in propanol by brush (11.85%), nanosilver in ethanol by brush (11.7%), and the sample treated with silver (9.5%).

These results indicated that the control sample had the lowest moisture content (5.8%), and the infected sample had the highest (13.3%). Additionally, different treatments with nanomaterials affected the internal water content of the samples differently, with nanochitosan by brush, showing the highest moisture content (12.7%) compared to the other samples (Table 7).

Field Emission Scanning Electron Microscopy (FESEM)

The surface morphological properties of the produced samples were investigated. Using a scanning electron microscope [38]. Figure 2 displays the distribution and morphology of the original and treated wood. The transverse sections of pine wood seen in the FESEM photos exhibit a high concentration of spherical nanoparticles on the wood's cell wall, causing the cell wall to become uneven. Woody plants' secondary tissues are made up of stiff cell walls and brittle cells. However, when mechanically cross-sectioned for electron microscope investigation, the structures are easily destroyed [39].

Morphological Observation

A thorough visual portrayal of the surface morphology in several samples, including the control sample, treated, and infected samples, is given by the SEM images shown in Figure 18. Wood's intrinsic anisotropic properties are typified by interconnecting cellular structures (Fig. 18a). Wood has alternating patterns of ridge-like protrusions (cell walls) and groove-like depressions (cell cavities) in its longitudinal section and a honeycomb-like structure in its cross-

section. The cell surfaces are frequently smooth and densely packed in natural wood that has not deteriorated [40].

SEM images of the standard sample showed clear, well-defined, and well-preserved cross-sectional images of tracheids (Fig. 18a), while the infected sample showed clear fungi on the outer surface. The infected sample showed hyphae. It was found as fine filaments interspersed among the wood cells (Fig. 18b-c), invading the cell walls. It led to the breakdown of wood cell walls as the fungi penetrated, and the spores visible appeared as small, round structures scattered throughout the wood matrix. Samples treated with nano-chitosan (Fig. 18d-e), showed that the sterilizing material was applied twice to the surface to ensure complete inhibition of microbial growth on the surface. The calcification of the material on the surface of the treated wood sample illustrated its penetration into the tracheids. The sample treated with silver in ethanol by spray (Fig. 18f) showed that the tracheids were filled with disinfectant, and when applied with a brush (Fig. 18g), the tracheid lumens were sealed off [41].

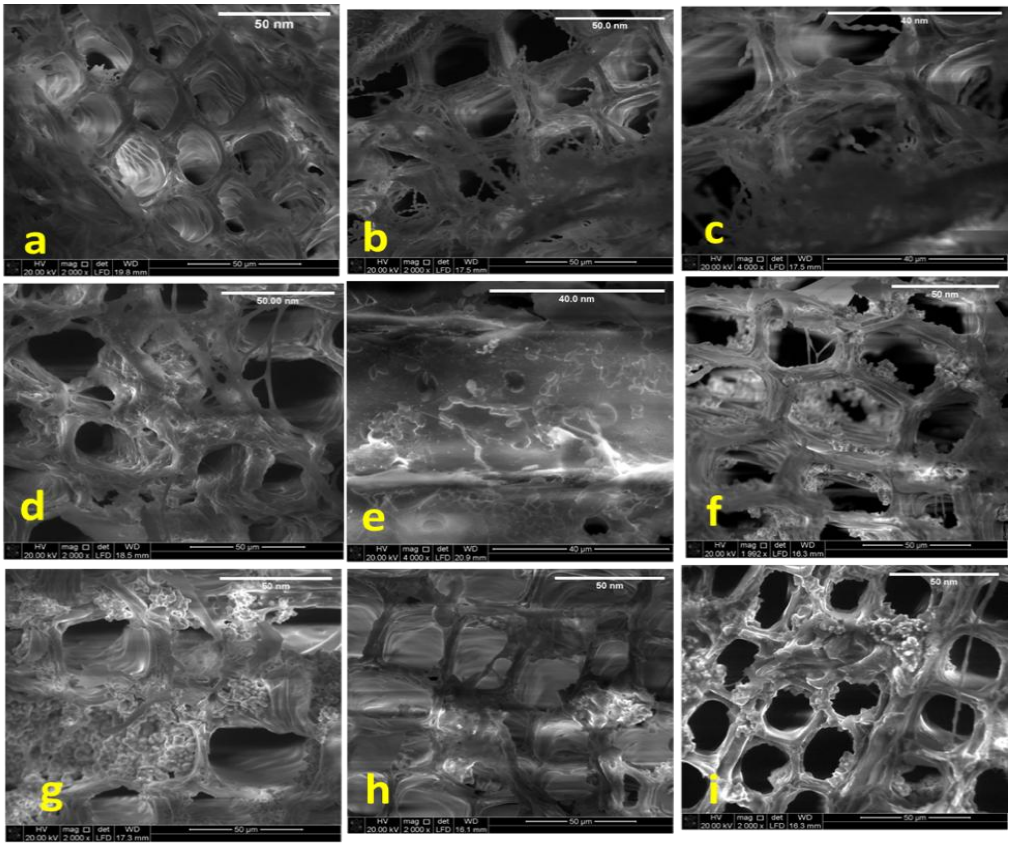

Fig. 18. FESEM of the wooden sample: a) Control b) & c) Infected; d) CS NP by spray; e) CS NPS by brush; f) AgNp in ethanol by spray; g) Ag-Np in ethanol by brush; h) Ag Np in propanol by spray; i) AgNp in propanol by spray

Surface 3D topographic images of the control and treated samples showed that the surface of all samples was not completely flat; 50 nm SEM images were used to compare the results. Similarly, SEM images at the same magnification of 50 nm were used to assess the control, infected, and treated samples equally. The control sample was observed to show less change in the surface shape compared to the infected and treated samples. This also depends on the level of the sample surface before infection and treatment, as well as the effect of the

fungi on the wood surface, the treatment material, and the extent of its calcification on the surface (Fig. 19).

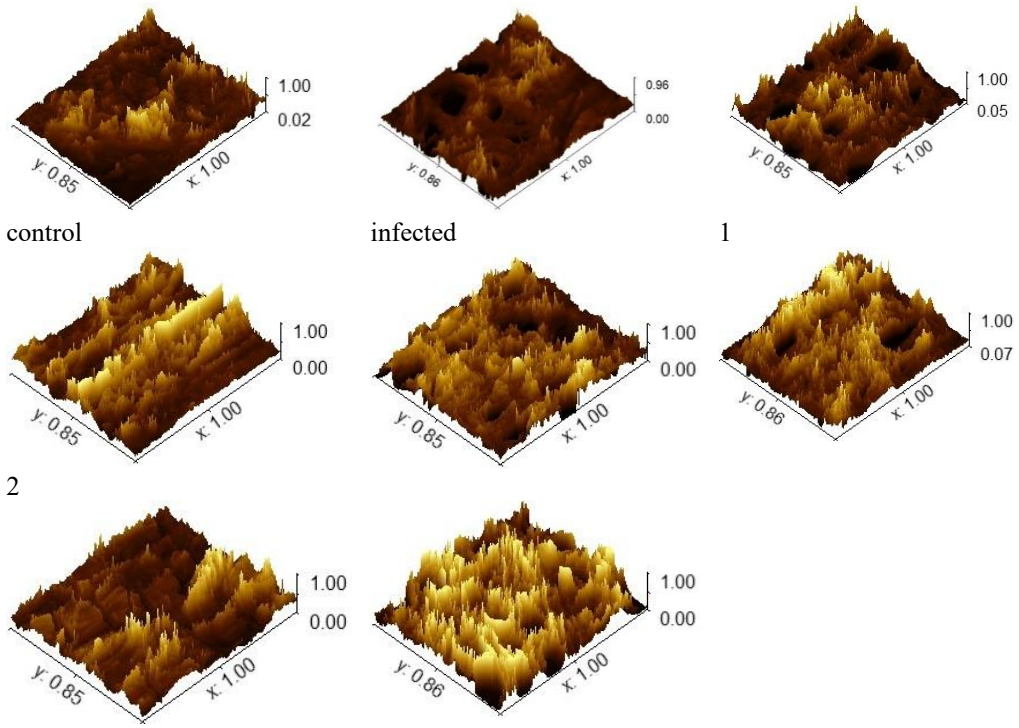

Fig. 19. 3D topographic images of the surface of the wooden samples: a) Control b) Infected; c) CS NPS by spray; d) CS NPS by brush; e) Ag-Np in ethanol by spray; f) Ag NPS in ethanol by brush; g) Ag NPS in propanol by spray; h) Ag NPS in propanol by spray

Analysis of Energy-Dispersive Spectroscopy (EDS)

Figure 20 displays the results of the EDS analysis used to identify the chemical elemental compositions of the Ag wood-based nanocomposites and the original wood. The presence of the element Ag was plainly observed, indicating that Ag had been successfully deposited onto the hardwood samples' surface. It was determined that the mass percentage of Ag on the surface of the wooden samples was 96.1% based on the Ag elemental mass percentage.

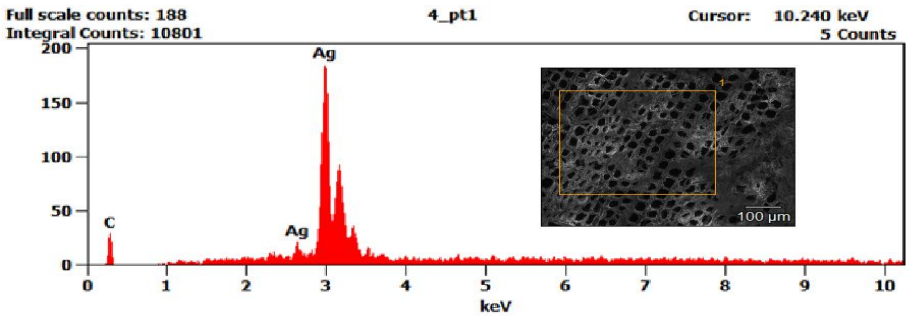

Fig. 20. SEM-EDX spectrum of the wooden sample after treatment by nanosilver (2%)

Ag Distribution

Figure 20 displays the findings of the EDS analysis used to determine the chemical elemental compositions of the original wood and the Ag wood-based nanocomposites. Ag could

be readily seen, indicating that it had been successfully deposited into the hardwood samples' surfaces. It was determined that the mass percentage of Ag on the wooden surface was 15.33% based on the Ag elemental mass percentage.

FTIR Examination

FTIR spectra were used to characterize the chemical functional groups on the wood's surface before and after treatment (Fig. 5). A large and powerful vibrational signal at 3350 cm^{-1} was seen in the control sample, indicating the presence of hydrophilic–OH functional groups in wood.

FTIR Analysis of the Control and Infected Wooden Samples

FTIR analysis of wood in Fig. 21 showed that most changes occurred in the chemical compounds between the control and infected samples. The infrared spectrum showed some change in the functional groups between the standard sample and the infected sample due to fungal degradation, which was caused by the breaking of cellulose chains, depolymerization, and loss of lignin. In contrast, the other samples treated with nanomaterials had a slight change in the functional groups.

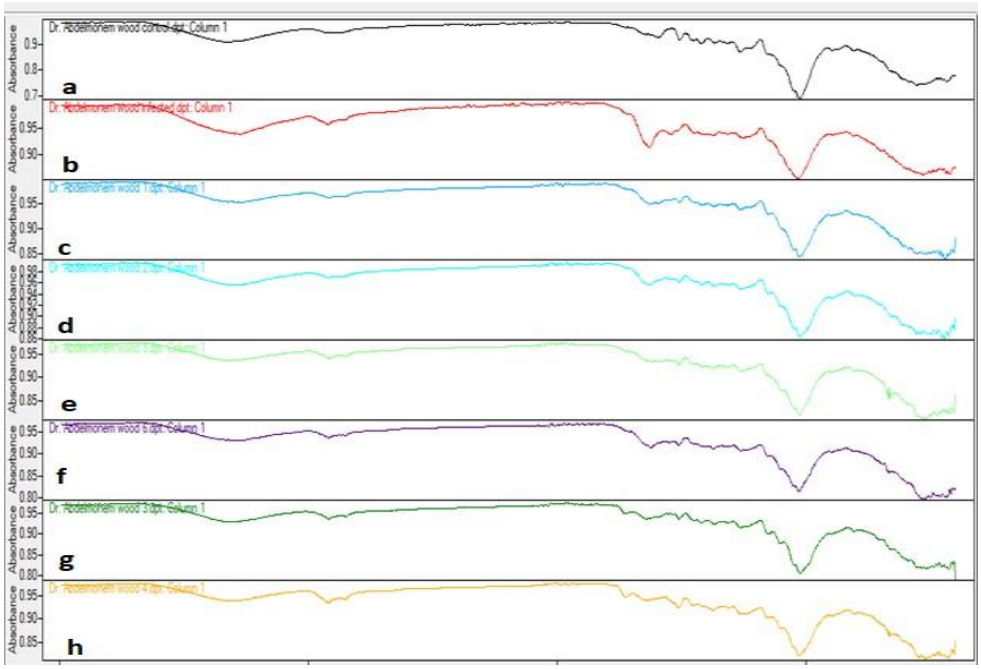

Fig. 21. Fourier transform infrared spectroscopy (FTIR) of the wooden samples; a) Control b) Infected; c) CS NP by spray; d) CS NPS by brush; e) Ag-Np in ethanol by spray; f) Ag-Np in ethanol by brush; g) Ag Np in propanol by spray; h) AgNp in propanol by spray

The infected sample increased the intensity band of water absorption around 1637 cm^{-1} and raised the O-H stretching band around 3244-3331 cm^{-1} (Fig. 21b) because of the acquisition of water due to the humidity used for the growth of fungi.

The infected samples illustrated that the 3341 cm^{-1} band corresponded to the O-H stretching in cellulose, lignin, and hemicellulose; 3244 cm^{-1} corresponded to the O-H stretching in cellulose; and 2920 cm^{-1} corresponded to the C-H_2 asymmetric stretching in cellulose, lignin, and hemicellulose. Additionally, the 2850 cm^{-1} denoted the C-H_2 symmetric stretching in cellulose, lignin, and hemicellulose. The 1720 cm^{-1} band denoted the unconjugated C=O stretching as a shoulder for xylan and hemicellulose, which was ascribed to holocellulose and decreased gradually. Moreover, the 1633 cm^{-1} showed the conjugated C=O stretching + H-O-H absorption due to the oxidation of cellulose. The 1545 cm^{-1} band corresponded to the C=C stretching of the aromatic ring of lignin, while the 1460 cm^{-1} band denoted the CH_3 bending of

cellulose, lignin, and hemicellulose. The 1423 cm^{-1} band corresponded to the CH_2 bending of cellulose (crystallized and amorphous), the 1379 cm^{-1} band denoted the CH_2 bending of cellulose, the 1266 cm^{-1} corresponded to the C-O stretching of lignin (guaiacyl), the 1222 cm^{-1} band corresponded to the C-O stretching of lignin (syringyl), and the 895 cm^{-1} band denoted the C-H aromatic bending out of plane + C-H rocking of lignin and cellulose [42-48].

The samples treated by nanochitosan by brush and spray gave the same result of 2927 cm^{-1} C-H_2 asymmetric stretching of cellulose, lignin, and hemicellulose. The 2846 cm^{-1} band corresponded to the C-H_2 symmetric stretching of cellulose, lignin, and hemicellulose. Additionally, 1627 cm^{-1} denoted the conjugated C=O stretching + H-O-H absorption due to the oxidation of cellulose; 1597 cm^{-1} denoted the C=C stretching of the aromatic ring of lignin (syringyl > guaiacyl); 1506 cm^{-1} denoted the C=C stretching of the aromatic ring for lignin; 1413 cm^{-1} denoted CH_2 bending of cellulose (crystallized and amorphous); 1376 cm^{-1} denoted CH_2 bending of cellulose; 1319 cm^{-1} denoted OH bending + C-O stretching of cellulose (amorphous) + lignin (syringyl); 1270 cm^{-1} denoted C-O stretching of lignin (guaiacyl); and 891 cm^{-1} denoted C-H aromatic bending out of plane + C-H rocking for lignin + cellulose (Fig. 21 c and d).

The result of the samples treated by nanosilver with ethanol by spray was the same as with nanosilver in ethanol by brush except for the decrease in 1627-1593-1510 cm^{-1} C=C stretching of the aromatic ring lignin and 1593 and 1460 cm^{-1} CH_3 bending of cellulose, lignin, and hemicellulose. The 1423 cm^{-1} band denoted the CH_2 bending of cellulose (crystallized and amorphous); 1366 cm^{-1} denoted the CH_2 bending of cellulose; the 1313 cm^{-1} band indicated the OH bending + C-O stretching of cellulose (amorphous) + lignin (syringyl), except for the decrease in the 1643 cm^{-1} and 1590 cm^{-1} bands due to the oxidation of cellulose and lignin [49] (Fig. 21 e and f).

The samples treated with nanosilver and propanol by spray indicated 2927 cm^{-1} of the C-H_2 asymmetric stretching of cellulose, lignin, and hemicellulose and the 2856 cm^{-1} band of the C-H_2 symmetric stretching of cellulose, lignin, and hemicellulose. The 1727 cm^{-1} suggested the unconjugated C=O stretching as a shoulder for xylan and hemicellulose; the 1643 cm^{-1} band indicated the conjugated C=O stretching + H-O-H absorption due to the oxidation of cellulose; 1506 cm^{-1} denoted the C=C stretching of the aromatic ring for lignin; and 1461 and 1453 cm^{-1} denoted the CH_3 bending for cellulose, lignin, and hemicellulose. Furthermore, 1373 cm^{-1} suggested the CH_2 bending for cellulose; 1313 cm^{-1} denoted the OH bending and C-O stretching for cellulose (amorphous) and lignin (syringyl); and 1229 cm^{-1} indicated the C-O stretching for lignin (syringyl) (Fig. 21g).

The treated samples by nanosilver in propanol by brush indicated the 1730 cm^{-1} unconjugated C=O stretching as a shoulder for xylan and hemicellulose, 1650 cm^{-1} for the conjugated C=O stretching + H-O-H absorption due to cellulose oxidation, 1260 cm^{-1} C-O stretching of lignin (guaiacyl), and 1100 cm^{-1} C-O stretching of cellulose and hemicellulose (Fig. 21h).

Mechanical properties

Due to the limited number of samples, the mechanical properties test was conducted longitudinally because it is the direction that has the most loads in the wooden ceiling. Since wood is prone to mold growth in moist situations, its mechanical qualities are also diminished, and its aesthetic and ornamental qualities are negatively impacted by dense mold growth [50]. There is a considerable amount of molecular porosity in the wood cell walls. The primary drive behind the application of nanotechnology in wood science and technology is the special ability of nano-based materials to enter wood substrates deeply, changing the surface chemistry of the wood in the process [51]-[54].

The results of the mechanical properties test indicated that the standard sample measured 2623.83 N, while the infected samples measured 3476.44 N. The treated sample with nanochitosan applied by spray measured 6800.23 N, followed by the sample treated with nanosilver in ethanol by brush (5128.705 N) and nanosilver in propanol applied by brush, which measured 3888.162 N, followed by nanosilver in propanol by spray 3544.305 N and nanosilver in ethanol by spray (2305.486 N). The sample with the lowest mechanical properties was treated with nanosilver in ethanol by spray, measuring 2305.486 N (Table 8).

Table 8. Results of the mechanical properties test

No	Sample	Force N	Max stress N/mm²	Displacement (mm)
1	Control	2623.83	7.1444	5.8261
2	Infected	3476.44	29.6343	16.2097
3	Nano-Chitosan by spray	6800.23	28.15	13.566
4	Nano-Chitosan by Brush	2553.60	21.1334	13.199
5	Nano-Silver Ethanol by spray	2305.486	29.6361	7.657
6	Nano-Silver Ethanol by Brush	5128.705	29.6364	7.657
7	Nano-Silver propanol by spray	3544.305	29.6379	16.706
8	Nano-Silver propanol by Brush	3888.162	29.6357	16.706

Conclusion

The main goal of the current study was to determine the antimicrobial properties of some materials tested on the isolated fungi and bacteria from the cavern beneath the National Police Museum, evaluate nanomaterials used to inhibit microbial growth on ancient wood with different solvents, and apply them using a brush or spray method. The bacteria were *Micrococcus lutus*, *Streptomyces vinaceus, Microbacterium imperial*, *and Kacurin turfanensis* ,while the fungi were *Aspergillus niger, Humicola fuscoatra, Alternaria alternata, and Penicillium oxalicum.* Nanosilver (Ag NP), nanosilica (SiO_2 NP), and titanium dioxide (TiO_2 NP) were used at a concentration of 2% in different solvents, such as distilled water, ethanol, propanol, and butanol. Nanochitosan CS NP was used with water only. The result showed that nanochitosan had the highest fungal inhibition (30 mm) for all isolated microbial organisms. It was followed by Ag Np in ethanol and Ag Np in propanol, which affected all microbial organisms and gave a negative result for *Penicillium oxalicum* and *Humicola fuscorta*. The moisture content of the standard sample was 5.8%, while it ranged between 9.45% and 13.3% for the treated samples.

The surface morphological properties of the produced samples were investigated by FESEM. SEM showed the nanomaterials calcified on the surface due to their application twice to obtain the best growth inhibition. Surface 3D topographic images of the control and treated samples showed that the surface of all samples was not completely flat, as shown by Gwyddion software. FTIR illustrated the functional group change between the infected and the treated samples. The results of the mechanical properties test indicated that the treated sample with nanochitosan applied by spray measured the highest mechanical properties at 6800.23 N; the sample with the lowest mechanical properties was the one treated with nanosilver in ethanol by spray, measuring 2305.486 N.

References

[1] P. Svora *et al*., “Study of interactions between titanium dioxide coating and wood cell wall ultrastructure,” *Nanomaterials*, vol. 12, no. 15, art. no. 2678, 2022. DOI: 10.3390/nano12152678.

[2] G. Abdel-Maksoud, M. Abdel-Nasser, S. E.-D. Hassan, A. M. Eid, A. Abdel-Nasser, and A. Fouda, “Biosynthesis of titanium dioxide nanoparticles using probiotic bacterial strain, *Lactobacillus rhamnosus*, and evaluation of their biocompatibility and antifungal activity,” *Biomass Conversion and Biorefinery*, vol. 14, no. 19, 2024, pp. 23961–23983. DOI: 10.1007/s13399-023-04587-x.

[3] A. N. Papadopoulos and G. Z. Kyzas, "Nanotechnology and wood science," *Interface Science and Technology*, pp. 199-216, 2019. DOI: 10.1016/b978-0-12-814178-6.00009-1.

[4] M. Othman, H. Saada, and Y. Matsuda, “Antifungal activity of some plant extracts and essential oils against fungi-infested organic archaeological artifacts," *Archaeometry*, vol. 62, no. 1, pp. 187–199, 2020. DOI: 10.1111/arcm.12500.

[5] D. A. Avdanina and A. A. Zhgun, “Rainbow code of biodeterioration to cultural heritage objects,” *Heritage Science*, vol. 12, no. 1, art. no.187, 2024. DOI: 10.1186/s40494-024-01298-y.

[6] H. A. M. Afifi, M. M. A. Mansour, A. G. A. I. Hassan, and M. Z. M. Salem, "Biodeterioration effects of three *Aspergillus* species on stucco supported on a wooden panel modeled from Sultan al-Ashraf Qaytbay Mausoleum, Egypt," *Scientific Reports*, vol. 13, no. 1, art. no. 15241, 2023. DOI: 10.1038/s41598-023-42028-x.

[7] G. Abdel-Maksoud and M. Ismail, "Analytical methods for studying mummification technique and degradation process of a human mummy from the late period," *Journal of Cultural Heritage*, vol. 68, pp. 237–245, 2024. DOI: 10.1016/j.culher.2024.06.007.

[8] A. M. Abdelmoniem *et al*., "Conservation processes of a wooden coffin covered with a black resin layer and colored materials in Dahshur archaeological area," *International Journal of Conservation Science*, vol. 14, no. 4, pp. 1485–1506, 2023. DOI: 10.36868/IJCS.2023.04.16.

[9] M. Lazari and F. Elmi, "Structural study of coated wood with superhydrophobic chitosan/silica hybrid nanocomposite in seawater," *Progress in Organic Coatings*, vol. 186, art. no. 108076, 2024. DOI: 10.1016/j.porgcoat.2023.108076.

[10] A. Ślosarczyk, I. Klapiszewska, D. Skowrońska, M. Janczarek, T. Jesionowski, and Ł. Klapiszewski, "A comprehensive review of building materials modified with metal and metal oxide nanoparticles against microbial multiplication and growth," *Chemical Engineering Journal*, vol. 466, Article Number: 143276, 2023. DOI: 10.1016/j.cej.2023.143276.

[11] A. Abdelmoniem, N. Mahmoud, S. Mohamed, M. Abdel-Fatah, M. Mohammad, and N. Badr, "Multidisciplinary approach for documentation of an anthropoid wooden coffin from the late period in Egypt," *Advanced Research in Conservation Science*, vol. 3, no. 2, pp. 15–26, 2022. DOI: 10.21608/arcs.2022.136413.1026.

[12] R. Bansal, H. C. Barshilia, and K. K. Pandey, "Nanotechnology in wood science: Innovations and applications," *International Journal of Biological Macromolecules*, vol. 262, art. no. 130025, 2024. DOI: 10.1016/j.ijbiomac.2024.130025.

[13] N. S. Geweely, "New frontiers review of some recent conservation techniques of organic and inorganic archaeological artefacts against microbial deterioration," *Frontiers in Microbiology*, vol. 14, Article Number: 1146582, 2023. DOI: 10.3389/fmicb.2023.1146582.

[14] P. V. Alfieri and G. Canosa, *Nano-sustainable protective system to control biological colonization for wood heritage*, 15, 2023. DOI: 10.20944/preprints202306.1071.v1.

[15] J. Guo *et al*., "Molecular and crystal structures of cellulose in severely deteriorated archaeological wood," *Cellulose*, vol. 29, no. 18, pp. 9549–9568, 2022. DOI: 10.1007/s10570-022-04856-4.

[16] G. De Filpo, A. M. Palermo, F. Rachiele, and F. P. Nicoletta, "Preventing fungal growth in wood by titanium dioxide nanoparticles," *International Biodeterioration & Biodegradation*, vol. 85, pp. 217–222, 2013. DOI: 10.1016/j.ibiod.2013.07.007.

[17] D. E. Colbu, I. Sandu, V. Vasilache, K. Earar, E. D. Paraschiv, I. G. Sandu, D. B. Iliescu, and A. V. Sandu, "Study on the chemical composition of teak wood extracts in different organic solvents," *iForest-Biogeosciences and Forestry, v*ol. 14, pp. 329-336, 2021. DOI: 10.3832/ifor3717-014.

[18] A. M. Abdelmoniem *et al*., "Conservation of a painted wooden coffin at Dahshur archaeological area," *International Journal of Conservation Science*, vol. 15, no. 1, pp. 391–402, 2024. DOI: 10.36868/IJCS.2024.01.01.

[19] V. A. J. Jaques, E. Zikmundová, J. Holas, T. Zikmund, J. Kaiser, and K. Holcová, "Conductive cross-section preparation of non-conductive painting micro-samples for SEM analysis," *Scientific Reports*, vol. 12, no. 1, art. no. 19650, 2022. DOI: 10.1038/s41598-022-21882-1.

[20] H. Turkulin, L. Holzer, J. Sell, K. Richter, "Application of the ESEM technique in wood research: Part I. Optimization of imaging parameters and working conditions," *Wood and Fiber Science*, vol. 37, no. 4, pp. 552 – 564, 2005.

[21] A. M. Abdelmoniem, N. Mahmoud, M. Ahmed Abdel-Fatah, S. Mohamed, and N. M. Badr, "Multi analytical techniques of anthropoid wooden coffin from Egypt's late period," *International Journal of Conservation Science*, vol. 13, pp. 1087–1100, 2022.

[22] A. M. Abdelmoniem, N. Mahmoud, W. S. Mohamed, A. Y. Ewais, and A. Abdrabou, "Archaeometric study of a polychrome wooden coffin from 26th dynasty-Egypt," *Mediterranean Archaeology and Archaeometry*, vol. 20, no. 1, pp. 7–17, 2020. DOI: 10.5281/zenodo.3364825.

[23] R. de Abreu Neto, J. T. Lima, L. M. Takarada, and P. F. Trugilho, "Effect of thermal treatment on fiber morphology in wood pyrolysis," *Wood Science and Technology*, vol. 55, no. 1, pp. 95–108, 2021. DOI: 10.1007/s00226-020-01238-6.

[24] A. M. Abdelmoniem, "Preserving the wooden heritage of the National Police Museum: challenges and conservation strategies," J*ournal of Infrastructure Preservation and Resilience*, vol. 6, no. 1, p. 14, 2025. DOI: 10.1186/s43065-025-00117-3.

[25] P. Zanatta, M. Lazarotto, P. H. Gonzalez de Cademartori, S. da S. Cava, M. L. Moreira, and D. A. Gatto, "The effect of titanium dioxide nanoparticles obtained by microwave-assisted hydrothermal method on the color and decay resistance of pinewood," *Maderas. Ciencia y Tecnología*, 2017. DOI: 10.4067/S0718-221X2017005000901.

[26] F. Antonelli *et al*., "Essential oils as alternative biocides for the preservation of waterlogged archaeological wood," *Microorganisms*, vol. 8, no. 12, art. no. 2015, 2020. DOI: 10.3390/microorganisms8122015.

[27] F. Bartoli *et al*., "In situ evaluation of new silica nanosystems as long-lasting methods to prevent stone monument biodeterioration," *Coatings*, vol. 14, no. 2, art. no. 163, 2024. DOI: 10.3390/coatings14020163.

[28] A. Fouda *et al*., "An eco-friendly approach utilizing green synthesized titanium dioxide nanoparticles for leather conservation against a fungal strain, *Penicillium expansum* AL1, involved in the biodeterioration of a historical manuscript," *Biology*, vol. 12, no. 7, art. no. 1025, 2023. DOI: 10.3390/biology12071025.

[29] I. C. A. Sandu, M. Hayashi, V. Vasilache, D. G. Cozma, S. Pruteanu, M. Urma, I. Sandu, "Influence of Organic Solvents and Dispersions on Wooden Supports of Paintings," *Revista de Chimie,* vol. 66, no. 4, pp. 587-595, 2015.

[30] V. K. Mourya and N. N. Inamdar, "Chitosan-modifications and applications: Opportunities galore," *Reactive and Functional Polymers*, vol. 68, no. 6, pp. 1013–1051, 2008. DOI: 10.1016/j.reactfunctpolym.2008.03.002.

[31] P. Zanatta *et al*., "Exposure of *Pinus elliottii* wood treated with titanium dioxide to the fungus *Postia placenta* and photodegradation," *Madera y Bosques*, vol. 28, no. 1, art. no. e2811895, 2022. DOI: 10.21829/myb.2022.2811895.

[32] L.-F. Qi, Z.-R. Xu, Y. Li, X. Jiang, and X.-Y. Han, "In vitro effects of chitosan nanoparticles on proliferation of human gastric carcinoma cell line MGC803 cells," *World Journal of Gastroenterology*, vol. 11, no. 33, pp. 5136–5141, 2005. [Online]. Available: http://www.wjgnet.com/1007-9327/11/5136.asp

[33] A. Abdelmoniem, N. Mahmoud, M. Abd Elfatah, W. Mohamed, and A. Omar, "The impact of nanomaters on the microbial infection on a wooden coffin covered with a layer of black resin and coloured materials," *International Journal of Conservation Science*, vol. 15, no. 1, pp. 775–784, 2024. DOI: 10.36868/IJCS.2024.02.02.

[34] A. M. Omar, A. M. Abdelmoniem, F. El Wekeel, and A. S. Taha, "Spectroscopic and molecular investigation of Cheops wooden boat for microbial degradation applying proper," *Scientific Culture*, vol. 8, no. 1, pp. 115–127, 2022. DOI: 10.5281/zenodo.5717174.

[35] S. Hamed, S. A. M. Hamed, M. F. Ali, and N. M. N. El Hadidi, "Using SEM in monitoring changes in archaeological wood: A review," 2012. [Online]. Available: https://www.researchgate.net/publication/263350312

[36] A. M. Abdelmoniem, W. S. Mohamed, N. Mahmoud, M. A. Elfatah, and A. M. Omar, "Wooden coffin biodeterioration assessment and its restoration with different antimicrobial substances," *International Journal of Conservation Science*, vol. 13, no. 1, pp. 73–84, 2022.

[37] A. M. Abdelmoniem, N. Mahmoud, and W. S. Mohamed, “Isolation and characterization of microbial infection of polychrome wooden coffin from the 26th Dynasty, Egypt,” *Scientific Culture*, vol. 6, no. 3, pp. 1–6, 2020. DOI::10.5281/zenodo.3956802.

[38] S. Zheng, W. Tang, J. Tong, K. Cao, H. Yu, and L. Xie, “Innovative treatment of ancient architectural wood using polyvinyl alcohol and methyltrimethoxysilane for improved waterproofing, dimensional stability, and self-cleaning properties,” *Forests*, vol. 15, no. 6, art.no. 978, 2024. DOI: 10.3390/f15060978.

[39] T. Hatano, S. Nakaba, Y. Horikawa, and R. Funada, “A combination of scanning electron microscopy and broad argon ion beam milling provides intact structure of secondary tissues in woody plants,” *Scientific Reports*, vol. 12, no. 1, art. no. 9152, 2022. DOI: 10.1038/s41598-022-13122-3.

[40] D. Dogu, K. Tirak, Z. Candan, and O. Unsal, “Anatomical investigation of thermally compressed wood panels,” *BioResources*, vol. 5, no. 4, pp. 2640–2663, 2010. DOI: 10.15376/biores.5.4.2640-2663.

[41] X.-H. Zhang *et al*., “Molecular and cellular analysis of orange plants infected with Huanglongbing (citrus greening disease),” *Plant Growth Regulation*, vol. 92, no. 2, pp. 333–343, 2020. DOI: 10.1007/s10725-020-00642-z.

[42] Y. Zidan, N. N. M. El Hadidi, and M. F. Mohamed, “Examination and analyses of a wooden face at the museum storage at the faculty of archaeology, Cairo University," *Mediterranean Archaeology and Archaeometry*, vol. 16, no. 2, pp. 1–11, 2016,. DOI: 10.5281/zenodo.47538.

[43] S. S. Darwish, N. M. N. El Hadidi, and M. Mansour, “The effect of fungal decay on *Ficus sycomorus* wood,” *International Journal of Conservation Science*, vol. 4, no. 3, pp. 271–282, 2013.

[44] R. Md Salim, J. Asik, and M. S. Sarjadi, “Chemical functional groups of extractives, cellulose and lignin extracted from native *Leucaena leucocephala* bark,” *Wood Science and Technology*, vol. 55, no. 2, pp. 295–313, 2021. DOI: 10.1007/s00226-020-01258-2.

[45] V. Emmanuel, B. Odile, and R. Céline, “FTIR spectroscopy of woods: A new approach to study the weathering of the carving face of a sculpture,” *Spectrochimica Acta Part A: Molecular and Biomolecular Spectroscopy*, vol. 136, pp. 1255–1259, 2015. DOI: 10.1016/j.saa.2014.10.011.

[46] B. S. Gupta, B. P. Jelle, and T. Gao, “Application of ATR-FTIR spectroscopy to compare the cell materials of wood decay fungi with wood mould fungi,” *International Journal of Spectroscopy*, vol. 2015, pp. 1–7, 2015. DOI: 10.1155/2015/521938.

[47] B. S. Gupta, B. P. Jelle, P. J. Hovde, and J. Holme, “Characterization of wood mould fungi by FTIR—A valuable step for prediction of initiation of decay,” 2011. [Online]. Available: https://www.researchgate.net/publication/295076491

[48] X. Colom, F. Carrillo, F. Nogués, and P. Garriga, “Structural analysis of photodegraded wood by means of FTIR spectroscopy,” *Polymer Degradation and Stability*, vol. 80, no. 3, pp. 543–549, 2003. DOI: 10.1016/S0141-3910(03)00051-X.

[49] G. Li, A. Huang, T. Qin, and L. Huang, “FTIR studies of Masson pine wood decayed by brown-rot fungi,” *Spectroscopy and Spectral Analysis*, vol. 30, no. 8, 2010, pp. 2133–2136.

[50] A. N. Papadopoulos, “Nanotechnology and wood science,” *Nanomaterials*, vol. 13, no. 4, art. no. 691, 2023. DOI: 10.3390/nano13040691.

[51] A. N. Papadopoulos and H. R. Taghiyari, “Innovative wood surface treatments based on nanotechnology,” *Coatings*, vol. 9, no. 12, art. no. 866, 2019. DOI: 10.3390/coatings9120866.

[52] C. Luca and I. C. A. Sandu, “Research on the influence of the solvents used in the active preservation processes upon old painting supports with preparation layers. I. Chemical composition, thermal analysis and IR study of the old, soil wood supports,” *Revista de Chimie,* vol. 49, no. 9, pp.638-645, 1998.

Received: August 25, 2025
Accepted: April 22, 2026